IEEE *Access*

Two-Terminal Fault Location Method of Distribution Network Based on Adaptive Convolution Neural Network

JIEFENG LIANG[ID], TIANJUN JING, HUANNA NIU, AND JIANGBO WANG
College of Information and Electrical Engineering, China Agricultural University, Beijing 100083, China
Corresponding author: Jiefeng Liang (liangjiefeng_cau@163.com)

ABSTRACT When a single-phase ground fault occurs in a distribution network, it is generally allowed to operate with faults for one to two hours, which may lead to further development of the fault and even threaten the safe operation of the power system. Therefore, when a small current system has a ground fault, it must be quickly diagnosed to shorten the time of operation with fault. In this paper, an adaptive convolutional neural network (ACNN)-based fault line selection method is proposed for a distribution network. This method improves the feature extraction ability of the network by improving the pooling model. Compared with deep belief network (DBN), it can improve the accuracy of fault classification by 7.86% and reduce the training time by 42.7%. On this basis, the secondary fault location is identified using the principle of two-terminal fault location. In this research, fault data obtained by Simulink simulation is used as training set, and ACNN model is built based on TensorFlow framework. The analysis of results proves that the model has a high fault recognition rate and fast convergence speed. It can be used as an auxiliary hand for fault diagnosis in distribution networks.

INDEX TERMS Convolutional neural network, adaptive pooling model, two-terminal fault location, distribution network, single-phase ground fault.

I. INTRODUCTION

Distribution networks in China are characterized by complex structures, large scale, wide coverage, and frequent ground faults, and more than 80% of these faults are single-phase ground faults [1]. For a long time, most neutral points of the distribution network have been grounded by arc suppression coils or are ungrounded. When a single-phase ground fault occurs, the system is allowed to continue its operation with fault for two hours, which leads to a series of problems [2]. For instance, the non-grounded phase voltage will rise to $\sqrt{3}$ times the voltage during normal operation, the overvoltage of the single-phase ground fault easily forms a phase-to-phase short circuit, and the ground fault point may cause personal injury or death. Therefore, the above procedure no longer meets the requirement of safe and stable operation. A fast and accurate fault diagnosis method for single-phase ground fault should be proposed to shorten the time required by maintenance personnel to search for the fault, to improve

the reliability of the power supply and to reduce economic losses [3].

Presently, the main methods used for identifying single-phase ground fault location in distribution networks are the impedance [4], [5], S-injection [6], [7], traveling wave [8] and port fault diagnosis methods [9]. In addition, a fault location method for distribution network based on advanced genetic algorithm is proposed in [10]. This method has high fault tolerance and can be used in complex situations of multiple sources and multiple faults. However, this method cannot utilize the feedback information of the network promptly, and the search speed is slow. It requires more training time to obtain the precise solution. Besides, it struggles to solve the problem of large-scale computation. Reference [11] presents a unified matrix algorithm for fault section judgment and isolation of distribution automation system based on remote terminal unit (RTU). This method requires significant computation, and terminal fault judgment is limited to single power supply systems. Reference [12] proposes a phasor measurement unit (PMU)-based fault location method for multi-terminal transmission lines. It needs to transform the

The associate editor coordinating the review of this manuscript and approving it for publication was Canbing Li[ID].
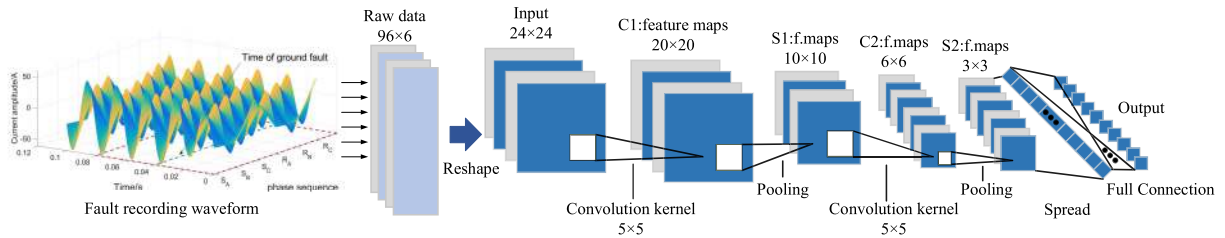
FIGURE 1. Network structure of CNN.

multi-terminal lines into equivalent three-terminal lines and further transform the fault location problem of three-terminal lines into two-terminal fault location. This method is greatly affected by the line structure, and there are large errors in the process of line transformation

In order to reduce the computation time, improve the search speed of fault location, reduce the influence of distribution network structure on the algorithm, and realize the fault location of the whole line without blind area, the convolutional neural network (CNN) is applied to the fault diagnosis of distribution network in this paper. With the development of computer technology, CNN as an artificial intelligence algorithm has been widely used in the research of power industry. A method for power quality disturbance classification is proposed by combining deep convolutional neural network with wigner-ville distribution [13]. Research on the application of deep learning in fault diagnosis of wind turbine gearbox and condition monitoring of wind turbine gearbox bearing highlight the excellent ability of deep learning in fault classification [14], [15]. Fault locations were defined as classification labels, and different CNN's were used to classify the labels to achieve the fault localization results. Then, image segmentation was performed to extract the features of fault areas and simplify the data volumes [16].

In this study, the authors proposed a distribution network fault location method combining ACNN with a two-terminal fault location method. This paper is organized as follows: section II introduces the generation of fault data set, the structure of ACNN, and the principle of adaptive pooling model. Section III describes the fault dataset used in the process of fault line selection and the principle of two-terminal fault location by negative sequence current. Finally, sections IV and V present the results and conclusions of the experiment generated during this research.

II. ACNN MODEL BASED ON FAULT RECORDING DATA
As a typical deep learning model, CNN improves the traditional machine learning system by relying on the three important ideas, namely sparse interaction, parameter sharing, and isotropic representation. It can realize feature extraction, classification model construction, and other functions through the training of input samples. It has made important progress in fault diagnosis [17]–[20]. In this study, the adaptive weight factor is added to the traditional CNN structure to improve

the convergence rate of the network and reduce the training time.

A. THE STRUCTURE AND PRINCIPLE OF CNN
Typical structures of CNN are mainly composed of the input layer, convolutional layer (C-layer), pooling layer (or sampling layer, S-layer), full connection layer, and output layer [21], as shown in Figure 1. Each sample is input in the form of a two-dimensional matrix, which is mapped to the hidden layer by the convolution kernel. The hidden layer is composed of a convolutional layer and a pooling layer. The C-layer and S-layer are set alternately to construct the sparse interaction between layers. CNN reduces the number of training parameters in this way. Additionally, through weight sharing, the S-layer fully preserves the local characteristics of data and reduces the dimension of data while preventing overfitting. By expanding all the outputs of the previous layer into a one-dimensional array, the affine layer connects all its neurons to integrate the local information with category differentiation in the C-layer or the S-layer. Finally, the output value of the affine layer is passed to the output layer.

Because of its unique network structure, CNN has a good ability to process data with network structure characteristics. Therefore, it can effectively solve the problem of difficult data processing caused by the complex structure, large scale, nonlinear, and other factors of a distribution network. It is suitable to process voltage and current data of single-phase ground faults in a distribution network and extract fault characteristics.

B. CONSTRUCTION OF INPUT FEATURE MAP
In this paper, the sampling data of a three-phase current at both ends of the line with two cycle before and two cycles after the fault is selected as the input. As shown in Figure 1, each phase current recorded data is taken as a column of the input feature map, and the size of the feature map is $4N_T \times 6$, where N_T is the number of sampling points in each cycle. The system parameters, fault location, system voltage, fault type, transition resistance, and other parameters are traversed in the form of permutation and combination. In this manner, the input feature map is formed, and the training sample set is constructed.

In addition, owing to the complex components of the fault transient [22], the collected fault recording data contains

high-frequency components and some random interference. Therefore, the input data needs to be smoothed properly to highlight the main part.

C. CONVOLUTION MODEL

The convolution process of the C-layer is shown in Figure 2. Its function is to extract local features of input neuron data. The size of the input feature map is $n \times n$ and is denoted by X. The size of the matrix with convolution kernel is $k \times k$ and that of the matrix with output denoted by Y is $m \times m$. The dimensional relation of the three is as follows [23].
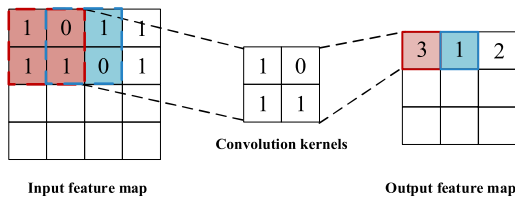
$$m = n - k + 1 \tag{1}$$

FIGURE 2. Principle diagram of convolution process.

The specific formula used for calculation is as follows:

$$Y_{ij} = f_s(\sum_{i=1}^{k} \sum_{j=1}^{k} (X_{ij}C) + a) \tag{2}$$

where X_{ij} and Y_{ij} are the elements corresponding to the convolution kernel of the input layer and output layer, a is the offset, and f_s is the sigmoid function.

The convolution process is used to extract the local characteristics of the current recording data at both ends of the fault line, which can be used to reduce the training parameters while representing the fault data.

D. ADAPTIVE POOLING MODEL

The pooling layer is a sub-sampling of the convolutional layer, whose purpose is to reduce the data dimension and prevent overfitting by scaling the output feature map of the previous layer. The pooling process is shown in Figure 3.
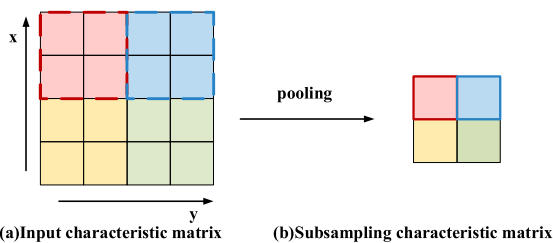
FIGURE 3. Principle diagram of pooling process.

The average and maximum pooling models, as the two most common pooling models, are widely used in the construction of neural networks. Their algorithm expressions are

shown as follows [23].

$$S_{ij} = \frac{1}{c^2}(\sum_{i=1}^{c} \sum_{j=1}^{c} F_{ij}) + b \tag{3}$$

$$S_{ij} = \max_{i=1, j=1}^{c} (F_{ij}) + b \tag{4}$$

Here, F is the input feature map, b is the bias, S is the sub-sampling characteristic matrix, and c is the size of the pooling matrix.

Because these two classical pooling models are insufficient for feature extraction of pooling domain [24], appropriate improvements should be made based on the classical pooling model to optimize the feature extraction process of the traditional CNN model. In this paper, adaptive weights are added on the basis of the maximum pooling model to optimize pooling results. The calculation is as follows [25]:

$$S_{ij} = \lambda \max_{i=1, j=1}^{c} (F_{ij}) + b \tag{5}$$

where λ is the adaptive weight factor, whose value is related to the number of network training layers and the element value in the pool domain. The formula for calculation is as follows:

$$\lambda = \alpha \frac{\bar{x}(x_{\max} - \bar{x})}{x_{\max}^2} + \beta \tag{6}$$

where $\bar{x}$ is the average value of elements other than the maximum value $x_{\max}$ in the pool domain, β is the compensation term, whose value range is (0, 1), α is the characteristic coefficient, calculated as follows:

$$\alpha = \frac{c}{1 + (n_{iter} - 1)c^{n_{iter}^2 + 1}} \tag{7}$$

where c is the size of the pool domain, n_{iter} is the number of CNN training, and *iter* is the number of times the training set is trained in the network. Therefore, the value of adaptive weight factor is not only related to the elements in the pool domain and its size, but also to the number of network training. In the test phase, when n_{iter} is set to 1, the pooling effect can be optimized by adjusting the edge length of the pooling domain. When the size of the pool domain is determined, the adaptive weight factor will be dynamically adjusted by increasing in the number of training times of the sample data set. Because of the adaptive pooling factor $\lambda \in (0, 1)$, the dynamic pooling model accounts for the two classical pooling models mentioned above. It not only retains the accuracy of the maximum pooling model when there is an obvious maximum eigenvalue in the pool domain, but also avoids the weakening of the maximum element.

III. THE PRINCIPLE OF FAULT LINE SELECTION AND LOCATION OF SINGLE-PHASE GROUND FAULT BASED ON ACNN

A. SINGLE-PHASE GROUND DIAGNOSIS MODEL BASED ON ACNN

In this paper, a fault line selection and location method based on ACNN is proposed for single-phase ground fault detection
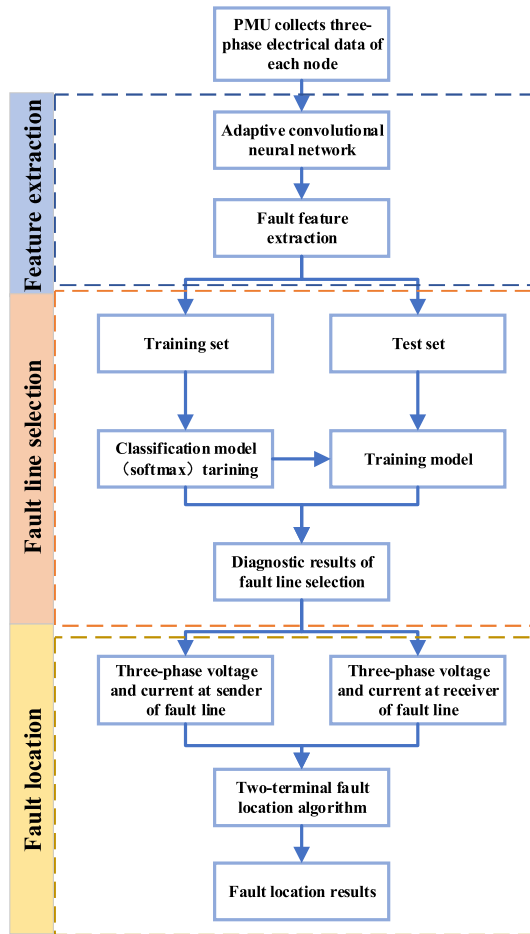
FIGURE 4. Principle Diagram of Fault Location Based on ACNN.

In the second part, the current phasor sampling data of each node of the line after feature extraction is divided into the training sample set and the test set. The training set is used to train the Softmax classifier. The test set is used to calculate the accuracy of ACNN network classification of the fault line after training. Through the calculation of loss function, when the error rate of test results is reduced to the allowable range, ACNN network parameters with high accuracy after training are saved.

The function of Softmax is

$$P(i) = \frac{\exp(\theta_i^T x)}{\sum_{k=1}^{K} \exp(\theta_k^T x)} \tag{8}$$

where x is the three-phase current characteristic data expanded after feature extraction of S2 layer, K is the classification number, and $P(i)$ is the probability belonging to class I.

Two SoftMax classifiers are set up in this study. They are respectively used for fault selection and fault judgment. This realizes the weight sharing of two different classification problems by the same network. Its classification labels are shown in Figure 5.

Function	The fault phase selection									Fault line	
Output	AN	BN	CN	ABN	BCN	CAN	AB	BC	CA	Internal	External
Labels	1	2	3	4	5	6	7	8	9	10	11

FIGURE 5. Fault classification index chart.

Set the number of output ports to 11. Labels 1 to 3 represent single-phase ground fault, labels 4 to 6 represent two-phase ground fault, and labels 7 to 8 represent phase to phase short circuit. For labels 10 to 11, set 1 for larger output and 0 for smaller output, respectively representing the internal and external fault of the line.

In the third part, when a single-phase ground fault occurs in the distribution network, fault current data of each node uploaded by PMU in real time are input into the trained ACNN model for fault line selection. When the fault line is determined, the fault record data of both ends of the fault line with the synchronization mark is called from the background, and the fault location algorithm is applied to locate the fault accurately.

B. TWO-TERMINAL FAULT LOCATION MODEL OF DISTRIBUTION NETWORK

To further determine the location of the fault, the two-terminal location principle is introduced. The schematic diagram is shown in Figure 6.

When a single-phase ground fault occurs in a distribution network, the fault power network can be divided into the positive sequence network, negative sequence network, and zero sequence network, according to the symmetrical component method and linear superposition principle. In this paper, the negative sequence voltage and current components at both ends of the fault line are used for fault location.

of distribution networks. The established model is shown in Figure 4. The model is divided into three parts: fault feature extraction, fault line selection, and fault location.

In the first part, PMU is used to obtain the current fault recording data of each node of the transmission line, and the synchronization time mark is added. After the smoothening process, it is input into the designed ACNN model for training. Then, the fault characteristics are extracted. Compared to the fault diagnosis method based on relative wavelet energy, the ACNN model proposed herein does not require complex operations such as wavelet decomposition of the original fault recorded data and calculation of relative wavelet energy to extract data features. During the training of the network, the model can automatically extract the features of the input data through the C-layer and the adaptive S-layer.

The number of hidden layers of ACNN is set according to the actual needs, through the analysis of the above input matrix dimensions and considering the dimensionality reduction effect of convolution and pooling processes. Therefore, in the process of model design, the number of hidden layer network layers is four, comprising two C-layers and two S-layers.

FIGURE 6. Equivalentnetworkdiagram of single-ended powersupply system.

FIGURE 7. The electrical topology of the 33-node distribution network.

TABLE 1. Parameters of faulty lines.

Faulty line	Length of line (km)	Total impedance of line (Ω)
L1	1.47	0.4930+j0.3969
L2	1.09	0.3660+j0.2949
L3	1.14	0.3811+j0.3072
L4	2.44	0.8190+j0.6601

TABLE 2. Traversal of fault data set parameters.

Parameter type	Parameter value	Parameter quantity
System frequency/Hz	49.5, 50, 50.5	3
system voltage/kV	9.9∠10°, 10.45∠15°, 11∠25°, 11.55∠35°, 12.1∠45°	5
Faulty line	L1, L2, L3, L4	4
Location of failure point/km	0.01, 0.2L, 0.3L, 0.4L, 0.5L, 0.6L, 0.7L, 0.8L, 0.9L, L -0.01	10
Transition resistance/Ω	0.01~1, 1~10, 10~50	10

When a single-phase ground fault occurs at point F of the line, the negative sequence voltage expression of the send terminal (S- terminal) and the receiver terminal (R- terminal) can be derived from reference [26] as follows:

$$U_{S2} = I_{S2}Z_2x + I_{F2}R_f + U_{F2} \qquad (9)$$
$$U_{R2} = I_{R2}Z_2(L-x) + I_{F2}R_f + U_{F2} \qquad (10)$$

where I_{S2}, I_{R2}, U_{S2} and U_{R2} are the negative sequence current phasor and voltage phasor of S and R terminals in case of single-phase ground fault, Z_2 is the negative sequence impedance of the line with unit length, x is the distance from the fault point F to the measuring point S, and L is the total length of the line.

By combining the two terms to the right of (8) and (9), they are further reduced to

$$U_{S2} = I_{S2}Z_2x + U_{FS2} \qquad (11)$$
$$U_{R2} = I_{R2}Z_2(L-x) + U_{FR2} \qquad (12)$$

where U_{FS2} and U_{FR2} are the negative sequence voltage phasor of the fault point calculated at the S-terminal and the R-terminal respectively.

When the data collected at both ends of the line are fully synchronized, the following equation can be obtained.

$$U_{FS2} = U_{FR2} \qquad (13)$$

With the development of GPS technology, the accuracy of the synchronous clock provided by GPS is within 1 μs. In other words, the phase angle measurement error in the power system can be less than 1° [27]. Therefore, it can be considered as synchronous sampling to collect voltage and current phasors at both ends of fault line with PMU.

Furthermore, the fault distance x under synchronous sampling data can be calculated from (10), (11), and (12).

$$x = \frac{|U_{S2} - U_{R2}| + I_{R2}Z_2L}{Z_2(I_{S2} + I_{R2})} \qquad (14)$$

IV. SIMULATION AND EXPERIMENT

In this study, the IEEE 33 node power distribution system is built in Simulink by MATLAB, and its system wiring diagram is shown in Figure 7. In the experiment, four lines L1 to L4 are selected to set different ground faults for the fault branch. The fault type is set by adjusting the fault module parameters.
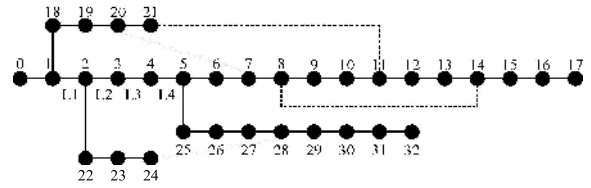
LJ-120 overhead line parameter, i.e. 0.335 + j0.27 Ω, is selected for the unit impedance of the line. The specific parameter settings are shown in Table 1.

In this paper, the sampling rate of the model is set to 1200 Hz; that is, the number of sampling points per cycle is 24. The PMU device is set at nodes Q1 to Q5. The fault points are set at different distances from line L1 to line L4, and the specific parameter settings are listed in Table 2.

Through parameter traversal, there are a total of 6000 sample data, which are input into the fault sample set. They are divided into the training and test sets via stratified sampling, with sizes of 1800 and 4200, respectively.

A. FAULT LINE SELECTION WITH ACNN
In this study, by setting different ACNN model structures, the accuracy of fault line selection and training time under

TABLE 3. Training results of single phase to ground fault line selection in distribution network based on ACNN.

NO.	Network structure	Convolution kernel	Amount of training per batch	Amount of testing per batch	Training times	Accuracy of classifier 1 /%	Accuracy of classifier 2 /%	Training time /s
1	1C-1S-C-1S	2 5	200	2000	1	17.00	19.36	1.19
2	1C-1S-C-1S	2 5	200	2000	1000	82.93	79.00	23.36
3	1C-1S-C-1S	1 1	200	2000	1000	80.90	76.50	23.01
4	1C-1S-C-1S	1 1	50	2000	1000	57.20	62.00	8.98
5	32C-1S-64C-1S	5 5	200	2000	2	87.00	90.26	2.69
6	32C-1S-64C-1S	5 5	200	2000	100	91.50	91.10	41.42
7	32C-1S-64C-1S	5 5	200	2000	1000	98.50	99.00	354.88
8	32C-1S-64C-1S	5 5	100	2000	1000	96.90	98.20	187.88
9	32C-1S-64C-1S	5 5	50	2000	1000	93.71	95.00	114.50
10	12C-1S-64C-1S	5 5	200	2000	1000	97.30	99.50	206.63
11	12C-1S-64C-1S	5 5	50	2000	1000	96.30	100.00	126.82
12	12C-1S-64C-1S	2 5	50	2000	1000	94.25	92.00	119.90
13	12C-1S-32C-1S	5 5	200	2000	1000	95.65	98.00	51.79
14	12C-1S-32C-1S	5 5	50	2000	1000	94.15	97.50	43.20

different network structures are obtained. The results of neural network training are listed in Table 3.

Table 3 is explained as follows. Take No. 1 as an example. The network structure parameter is set to 1C-1S-1C-1S, where C represents the convolution layer, S represents the pooling layer, and 1 represents the number of neurons in each layer. The two numbers in the convolution kernel are the convolution kernel sizes of the first convolution layer and the second convolution layer. 200 samples are entered into each batch during training. The accuracy of classifier 1 is the ratio of the successful fault phase selection samples to the total test samples. The accuracy of classifier 2 is the ratio of successful samples of fault judgment in and out of the area to the total number of test samples. Training time is the time required to complete the specified number of training times.

It can be seen from Table 3 that under the same data set, the structure of the network, the size of the convolution kernel, the amount of data processed in each training and the number of training will affect the accuracy of fault line selection. From the comparison of serial numbers 7, 8 and 9, it can be seen that under the same network structure, the more data each training process, the higher the accuracy. The comparison of 5, 6 and 7 shows that in the same network structure, the accuracy increases with the increase of training times, but when the training times reach a certain value, the accuracy keeps fluctuating near a certain value.

The experimental results show that the ACNN model performs best when the convolution kernel is 5 × 5 and structure is 32c-1s-64c-1s. The accuracy of fault line selection can

reach 98.50%, and the accuracy of fault judgment in and out of the area can reach 99%. In addition, it can be seen from the experiment that ACNN can still accurately select the fault line when the system frequency, fault location, system impedance, transition resistance and other factors are different. This is because the training sample data traverses the system parameters, and ACNN has strong generalization ability and learning ability. Through the learning of the training sample data, it is not affected by system parameters, fault location and other factors. Therefore, the more the number of samples, the more accurate the ACNN network for fault classification.

A fault location method based on the similarity and polarity of transient current between upstream and downstream is proposed [28]. Compared with this method, the ACNN model proposed in this paper can realize the fault line selection without blind area through multiple training. Figure 8 shows the zero-sequence current measured from node Q1 to Q4, when the fault point is near the outgoing line boundary point Q1. It can be seen from the above figure that the polarity of transient current in upstream and downstream of fault recording data is the same at some points. According to the method described in [28], line L1 will be misjudged as normal. By setting the fault location several times, the accuracy of fault line selection of this method and the ACNN model in the whole line is shown in Figure 9. It can be seen that the ACNN model proposed in this paper has a high fault identification ability for the whole section of the line. In addition, the recognition accuracy can be improved through secondary learning.
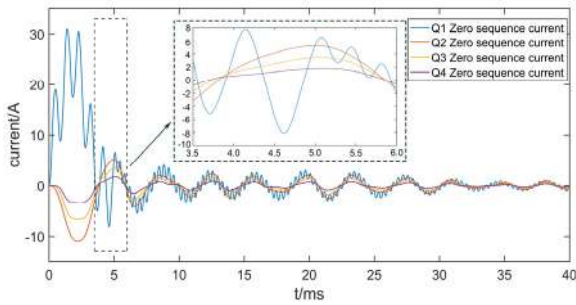
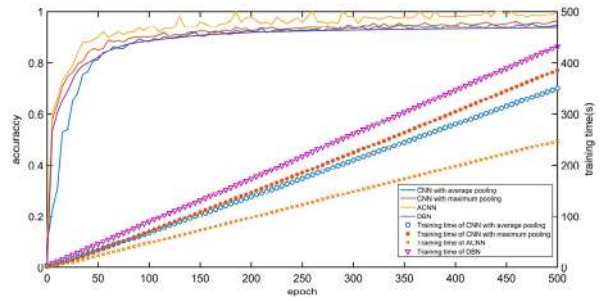**FIGURE 8.** Graph of the relation between the number of weight adjustments and mean square variance.

FIGURE 9. Comparison of fault line selection accuracy of different methods in different position faults.

B. ACNN VS CNN AND DEEP BELIEF NETWORK

In this section, ACNN is compared with traditional CNN and DBN in fault line selection. Figure 10 shows the relationship between the number of adjustment times of network structure parameters and the mean standard deviation of convolutional neural networks with different pooling models in the training process. It can be seen that the decreasing trend of the error value with the increase of the number of iterations is basically the same, but the convergence rate is different. The adaptive pooling model proposed in this paper has faster convergence speed. Because compared with the maximum pooling model and the average pooling model, the ACNN can achieve the optimal weight faster when adjusting the network parameters.

FIGURE 10. Graph of therelation between the number ofweight adjustments andmean square variance.

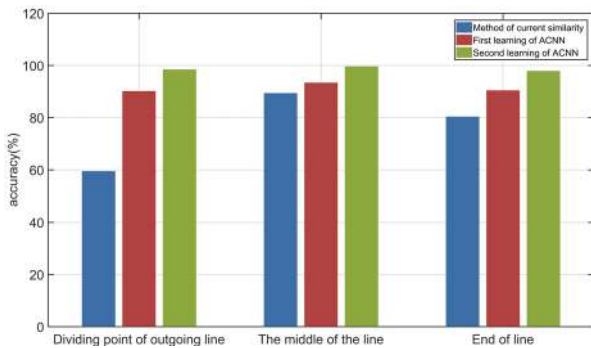**FIGURE 11.** Graph of therelation between the number ofweight adjustments andmean square variance.

TABLE 4. Accuracy rate and training time of each model with different iteration times.

Network type	Iteration	Accuracy	Time(s)
	50	0.9	23.42
ACNN	250	0.9580	122.7
	500	1	247.4
	50	0.8216	46.1
DBN	250	0.9231	217.3
	500	0.9271	431.8

The Figure 11 and Table 4 show that the ACNN model proposed in this paper has both the feature recognition accuracy of the maximum pooling model and the convergence speed of the average pooling model. Compared with the traditional DBN model, the proposed method reduces the time by 42.7% when the accuracy is increased by 7.86%.

C. FAULT LOCATION

After the fault line is determined, the fault point can be located by using (14). Through setting different types of faults at different positions of L1, the percentage of positioning error in the total line length was calculated, as shown in Table 5. The simulation results show that the proposed algorithm can eliminate the influence of load current, fault point transition resistance and system parameters. On the premise that the fault line and fault type are determined, the algorithm can locate the fault point accurately.

By setting metallic single-phase ground fault at different positions of line L1 to L4, the relationship between error and position can be calculated by applying the principle of two-terminal fault location, as shown in Figure 12. When the distribution network is powered by a single power supply, the positioning error increases as the distance of the fault location from the power supply. Through the analysis, it can be concluded that the error of fault location is within 7.6 m.

When the photovoltaic power supply is assembled on node 17, the relation between error and position is shown in Figure 12. By changing the connection node of photovoltaic equipment, it can be found that when there is photovoltaic
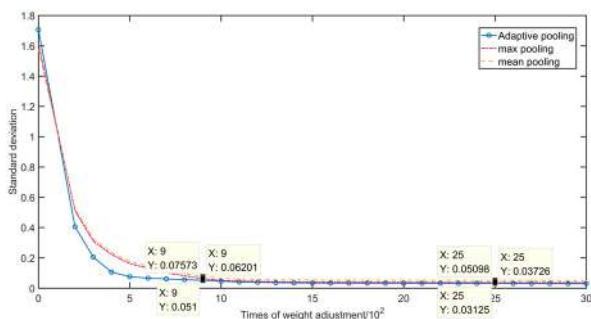
TABLE 5. Location results under different fault locations and transition resistances.

| Fault type	Fault location/km	Transition resistance/Ω	Location/km	Error/ (%)
AN	0.0735	10	0.0716	0.13
		50	0.0716	0.13
BN	0.0735	10	0.0716	0.13
		100	0.0716	0.13
CN	0.294	50	0.2896	0.30
		100	0.2896	0.30
ABN	0.294	50	0.2895	0.31
		200	0.2895	0.31
BCN	0.588	100	0.5823	0.39
		200	0.5823	0.39
CAN	0.882	50	0.8752	0.46
		500	0.8752	0.46
AB	0.588	100	0.5830	0.34
		1000	0.5830	0.34
BC	0.882	50	0.8757	0.43
		1000	0.8757	0.43
CA	0.882	50	0.8757	0.43
		100	0.8757	0.43
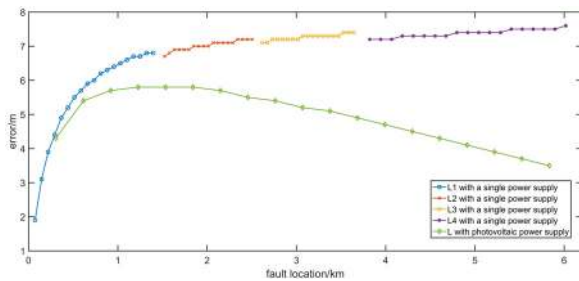
FIGURE 12. Fault location and location error diagram.

power in the distribution network, the changing trend of this curve is related to the connection node of photovoltaic equipment and the generation capacity. The overall error can be kept within 0.2% of the line length.

V. CONCLUSION

In this paper, a fault line selection method based on ACNN is proposed to solve the problem of fault detection during the operation of distribution system. The influence of different network structure parameters on the model line selection structure is analyzed. On this basis, combined with the principle of two-terminal fault location, the location error of different fault points is analyzed, and the relationship

between fault location error and different fault location is obtained. The simulation results show that the method has high accuracy of fault line selection and is less affected by system frequency, fault location, transition resistance, and other factors, and the experimental results are in agreement. In short distance transmission fault detection, the location error can be controlled within 7.6 m.

With the rapid development of computer software and hardware technology, ACNN will take less time to obtain samples, train weights and bias. The current data of each node with different fault types under different system parameters are obtained by simulation. Taking this as a sample, relying on ACNN's strong learning and generalization ability, it is expected to achieve accurate fault line selection for different power grids by using the same weight bias parameter. Finally, the fault is located by the principle of two-terminal fault location. The fault location method based on deep learning proposed in this paper has broad application prospects in the future development of smart grid.

REFERENCES

[1] S. Hou and W. Guo, "Fault line selection of distribution network based on improved phase-locked loop and chaotic oscillator," *Electr. Measur. Instrum.*, pp. 1–7, May 2019.

[2] X. Zeng, X. Yin, Y. Yu, and D. Chen, "A new method for control and protection of arc suppression coil grounding system based on injection variable frequency signal method," *Proc. CSEE*, vol. 1, pp. 30–33 and 37, 2000.

[3] P. Mao, Y. Sun, Z. Zhang, and H. Du, "Application of wavelet packet in single-phase earth fault line selection in distribution network," *Power Syst. Technol.*, vol. 6, pp. 9–13 and 17, 2000.

[4] N. Suo, J. Qi, F. Chen, G. Song, and Q. Xu, "Accurate fault location algorithm for transmission lines based on parameter identification of R-L model," *Proc. CSEE*, vol. 12, pp. 123–129, 2004.

[5] Y. Chen, J. Pei, X. Wang, S. Chen, B. Zhang, and Y. Yu, "Overview of fault location in distribution network," *Power Syst. Technol.*, vol. 18, pp. 89–93, 2006.

[6] X. Wang and Z. Sang, "A new method of fault location based on S injection method," *Relay*, vol. 7, pp. 9–12, 2001.

[7] T. Ji, T. Sun, Y. Xue, B. Xu, and P. Chen, "Current status and prospects of distribution network fault location technology," *Relay*, vol. 24, pp. 32–37, 2005.

[8] R. Zhang, Z. Chen, and G. Du, "Automatic localization algorithm for partial discharge of cable under oscillating wave voltage based on traveling wave method," *High Voltage Technol.*, vol. 45, no. 4, pp. 1289–1296, 2019.

[9] G. Cao, B. Zhu, and J. Jiang, "Virtual fault port method and its application in power system fault calculation," *Proc. CSEE*, vol. 5, pp. 43–49, 2002.

[10] Z. Wei, H. He, and Y. Zheng, "Advanced genetic algorithm for fault interval location in distribution network," *Proc. CSEE*, vol. 4, pp. 128–131, 2002.

[11] J. Liu, J. Ni, and Y. Du, "Unified matrix algorithm for fault segment judgment and isolation in distribution network," *Autom. Electr. Power Syst.*, vol. 1, pp. 31–33, 1999.

[12] B. Wang and Y. Zhou, "A new method for fault location of multi-terminal transmission lines based on PMU," *Power Syst. Prot. Control*, vol. 37, no. 12, pp. 32–35 and 39, 2009.

[13] K. Cai, W. Cao, L. Aarniovuori, H. Pang, Y. Lin, and G. Li, "Classification of power quality disturbances using Wigner-Ville distribution and deep convolutional neural networks," *IEEE Access*, vol. 7, no. 119, pp. 99–109, 2019.

[14] J. Fu, J. Chu, P. Guo, and Z. Chen, "Condition monitoring of wind turbine gearbox bearing based on deep learning model," *IEEE Access*, vol. 7, pp. 78–87, 2019.

[15] L. Lu, Y. He, T. Shi, and Y. Run, "Wind turbine planetary gearbox fault diagnosis based on self-powered wireless sensor and deep learning approach," *IEEE Access*, vol. 7, pp. 705–720, 2019.

[16] J. Duan, Y. He, B. Du, R. Ghandour, W. Wu, and H. Zhang, "Intelligent localization of transformer internal degradations combining deep convolutional neural networks and image segmentation," *IEEE Access*, vol. 7, pp. 430–442, 2019.

[17] T. Liang, J. Wang, H. Wang, and S. Wu, "Rolling bearing fault diagnosis using enhanced convolutional neural network with compressed sensing," in *Proc. Int. Conf. Sens., Diagnostics, Prognostics, Control (SDPC)*, Xi'an, China, Aug. 2018, pp. 148–152.

[18] Z. Zilong and Q. Wei, "Intelligent fault diagnosis of rolling bearing using one-dimensional multi-scale deep convolutional neural network based health state classification," in *Proc. IEEE 15th Int. Conf. Netw., Sens. Control (ICNSC)*, Zhuhai, China, Mar. 2018, pp. 1–6.

[19] Y. Du, Q. Shao, Y. Liu, G. Sheng, and X. Jiang, "Detection of single line-to-ground fault using convolutional neural network and task decomposition framework in distribution systems," in *Proc. Condition Monitor. Diagnosis (CMD)*, Perth, WA, USA, Sep. 2018, pp. 1–4.

[20] G. Jiang, H. He, J. Yan, and P. Xie, "Multiscale convolutional neural networks for fault diagnosis of wind turbine gearbox," *IEEE Trans. Ind. Electron.*, vol. 66, no. 4, pp. 3196–3207, Apr. 2019.

[21] F. Zhou, L. Jin, and J. Dong, "A review of convolutional neural networks," *Chin. J. Comput.*, vol. 40, no. 6, pp. 1229–1251, 2017.

[22] Q. Jia, L. Liu, Y. Yang, and J. Song, "Using wavelet to detect fault mutation to realize line selection protection of small current fault in distribution network," *Proc. CSEE*, vol. 10, pp. 79–83, 2001.

[23] D. Wei, Q. Gong, W. Lai, B. Wang, D. Liu, H. Qiao, and G. Lin, "Research on fault diagnosis and fault phase selection method in transmission line based on convolutional neural network," *Proc. CSEE*, vol. 36, no. S1, pp. 21–28, 2016.

[24] C. Hu, J. Qu, C. Xu, and A. Zhu, "Clothing image recognition based on adaptive pooling neural network," *J. Comput. Appl.*, vol. 38, no. 8, pp. 2211–2217, 2018.

[25] W. Liu, X. Liang, and H. Qu, "Study on learning performance of convolutional neural networks with different pooling models," *J. Image Graph.*, vol. 21, no. 9, pp. 1178–1190, 2016.

[26] J. Cui and A. Wang, "A novel fault location algorithm using double-ended electrical capacity," *Power Syst. Technol.*, vol. 12, pp. 17–19 and 27, 1996.

[27] S. Hu and X. Wang, "Synchronous phasor measurement device for power system based on GPS technology," *Electron. Eng.*, vol. 29, no. 11, pp. 21–23, 2003.

[28] Y. Xue, T. Li, W. Li, A. Hu, Z. Wang, and B. Xu, "A novel method of transient analysis and faulty section location for single-phase Earth fault in non-effectively Earthed network," *Autom. Electr. Power Syst.*, vol. 38, no. 23, pp. 101–107, 2014.

TIANJUN JING received the Ph.D. degree from the College of Information and Electrical Engineering, China Agricultural University, in 2011. He is currently an Associate Professor with the College of Information and Electrical Engineering, China Agricultural University. His current research interests include data mining of distribution networks and power system protection and control.

HUANNA NIU received the Ph.D. degree from the College of Information and Electrical Engineering, China Agricultural University, in 2012. He is currently an Associate Professor with the College of Information and Electrical Engineering, China Agricultural University. His current research interests include research of energy management and planning technology of distribution network and micro grid, distribution automation technology, power system operation, and planning and control.

JIEFENG LIANG received the B.S. degree from the Zhejiang University of Technology, Zhejiang, China, in 2017. He is currently pursuing the M.S. degree in electrical engineering with China Agricultural University, Beijing.

JIANGBO WANG received the Ph.D. degree from the College of Information and Electrical Engineering, China Agricultural University, in 2013. He is currently an Associate Professor with the College of Information and Electrical Engineering, China Agricultural University. His current research interests include power automation technology, microgrid operation control, and relay protection.

• • •